Adiabatic shaping of quadratic solitons

Lluis Torner and Carl Balslev Clausen*

Laboratory of Photonics, Department of Signal Theory and Communications, Universitat Politecnica de Catalunya, Gran Capitan UPC-D3, Barcelona, ES 08034, Spain

Martin M. Fejer

E. L. Ginzton Laboratory, Stanford University, Stanford, California 94305

Received January 26, 1998

We show the principle of operation of a setup to adiabatically shape solitons in quadratic nonlinear media to different beam profiles and widths or different fractions of energy carried by the second-harmonic wave. The shaping mechanism is based on soliton generation and propagation in chirped, quasi-phase-matched samples. © 1998 Optical Society of America

OCIS codes: 190.0190, 190.5530.

Optical solitons in quadratic nonlinear media[1–8] are a topic of current intense investigation. Interest in them is being fueled by new phenomena that are being uncovered and by potential applications of these solitons in signal routing and switching devices, in laser systems containing quadratic nonlinear crystals, and beyond.[2] For example, the unique features of solitons might open the possibility to use them in systems that require high-quality, well-controlled input signals, such as in some areas of biophotonics or in quantum devices.[6] Solitons in quadratic nonlinear media might be well suited for such purposes, because they form in both planar waveguides and bulk crystals and because they enjoy favorable amplitude–width relations that make them robust against small absorption losses and random perturbations. All applications might derive important benefits from the use of tailored signal shapes, and in some cases such shaping might just be crucial. Our goal in this Letter is to examine the properties of the solitons that form in chirped, quasi-phase-matched samples and to show the potential of such a geometry to shape the properties of the solitons in terms of beam profiles and widths or the fraction of the total energy flow that is carried by each of the waves that form the solitons.

The idea behind such behavior is similar to soliton pulse compression in dispersion-varying fibers[9] and is as follows. We consider soliton formation in a second-harmonic generation configuration so that the solitons form by the mutual trapping of fundamental-harmonic (FH) and second-harmonic (SH) waves. Solitons exist at different values of the wave-vector mismatch between both waves, but their properties are significantly different at each value of the mismatch. In particular, the soliton shapes and related features depend strongly on the value of the wave-vector mismatch as well as on the light intensity.[7,8] Quasi-phase-matching (QPM) techniques rely on the periodic modulation of the nonlinear properties of the medium to compensate for the existing wave-vector mismatch between the waves.[10] In the simplest QPM a constant period is ideally maintained over the whole length of the sample. In chirped QPM the period of the modulation is varied along the sample,[11] hence yielding a longitudinally varying wave-vector mismatch. The ability of solitons to adapt themselves adiabatically to the local wave-vector mismatch that they experience allows shaping of the output beams in samples with properly tailored chirps. Our aim here is to examine the process numerically and to identify suitable conditions for its implementation.

We consider spatial solitons in planar waveguides, but the analysis can be extended to soliton propagation in bulk media and to temporal solitons. The normalized evolution equations for the slowly varying envelopes of cw light beams in a quadratic nonlinear medium under conditions for type I QPM SH generation can be written as[1–8]

$$i\frac{\partial a_1}{\partial \xi} - \frac{r}{2}\nabla_\perp{}^2 a_1 + d(\xi)a_1{}^* a_2 \exp(-i\beta_0\xi) = 0\,,$$

$$i\frac{\partial a_2}{\partial \xi} - \frac{\alpha}{2}\nabla_\perp{}^2 a_2 + d(\xi)a_1{}^2 \exp(i\beta_0\xi) = 0\,, \qquad (1)$$

where a_1 and a_2 are the normalized amplitudes of the FH and the SH waves, respectively, $r = -1$, and $\alpha = -k_1/k_2$. Here $k_{1,2}$ are the linear wave numbers at each frequency. In all cases $\alpha \simeq -0.5$. The parameter β_0 is the normalized wave-vector mismatch given by $\beta_0 = k_1\eta^2\Delta k$, where $\Delta k = 2k_1 - k_2$ and η is beam width. The transverse coordinates are given in units of η, and the scaled propagation coordinate is $\xi = z/2l_{d1}$, where $l_{d1} = k_1\eta^2/2$ is the diffraction length. A beam width $\eta \sim 15$ μm and $\lambda \sim 1$ μm yield $l_{d1} \sim 1$ mm, and hence $\xi = 10$ corresponds to ~2 cm. The function $d(\xi)$ describes the periodic sign reversal of the nonlinear coefficients at given multiples of the coherence length $l_c = \pi/|\Delta k|$ involved in the QPM technique. Typical materials and operating wavelengths give coherence lengths in the range 2–20 μm. For the above values of the involved parameters a coherence length of ~10 μm corresponds to $|\beta_0| \sim 10^2$–10^3. These are the conditions encountered, e.g., in the QPM of the diagonal d_{33} nonlinear coefficient of $LiNbO_3$ at $\lambda \simeq 1.55$ μm.

0146-9592/98/120903-03$15.00/0

We consider a general chirped first-order QPM and expand $d(\xi)$ into its Fourier series:

$$d(\xi) = \exp\left(-i \sum_{\nu=1}^{\infty} D_\nu \xi^\nu\right) \sum_{n=-\infty}^{\infty} C_n \exp(inq_0\xi), \quad (2)$$

where $q_0 = 2\pi/\tau_0$ is the spatial frequency of the unchirped QPM; $\tau_0 = 2\pi/|\beta_0|$ is the normalized period of the unchirped QPM; C_n are the Fourier expansion coefficients of the unchirped QPM, given by $C_{2n} = 0$ and $C_{\pm(2n+1)} = \pm 2/[i\pi(2n+1)]$; and D_ν are the coefficients of the chirps. The local QPM period is

$$\tau(\xi) = \tau_0 \frac{|\beta_0|}{|\beta_0| - \sum \nu D_\nu \xi^{\nu-1}}. \quad (3)$$

Here we assume that all $D_\nu = 0$, except D_1 and D_2. Physically, when $D_1 > 0$ and $D_2 < 0$, this corresponds to a sample whose domain lengths at $\xi = 0$ are longer than τ_0 and down the sample become shorter.

Substitution of the above expressions into Eqs. (1), averaging out over the periodic fast varying terms and keeping only the lowest-order terms, gives[12,13]

$$i\frac{\partial a_1}{\partial \xi} - \frac{r}{2}\nabla_\perp{}^2 a_1 - i\frac{2}{\pi} a_1{}^* a_2 \exp[-i\beta(\xi)\xi] \simeq 0,$$

$$i\frac{\partial a_2}{\partial \xi} - \frac{\alpha}{2}\nabla_\perp{}^2 a_2 + i\frac{2}{\pi} a_1{}^2 \exp[i\beta(\xi)\xi] \simeq 0, \quad (4)$$

with $\beta(\xi) = D_1 + D_2\xi$. Therefore, under the conditions in which Eqs. (4) hold, the chirped QPM geometry is equivalent to a type I phase-matching setup with a longitudinally varying wave-vector mismatch.

The potential of the chirped QPM samples as shaping devices is based on the dependence of the soliton properties on the mismatch.[7,8] Stable solitons exist at all values of β. For a given mismatch and beam width, solitons exist above a threshold light intensity. The threshold increases with the mismatch. At positive β the solitons are constituted by a large FH and a small SH; the larger the mismatch, the smaller the SH. Near phase matching, the SH is comparable with the FH. At negative β the SH becomes the largest. Figure 1(a) shows the fraction of the total energy flow $I = \int(|a_1|^2 + |a_2|^2)\mathrm{d}r_\perp$ carried by each of the waves as a function of β for two values of I. For a given I the solitons are wider at large β and narrower near phase matching, as shown in Fig. 1(b). With these features in mind, the idea is to consider a variation of the mismatch such that a soliton is formed at the beginning of the sample after a short transient and that at the end of the sample the local mismatch gives the desired soliton shape. The question is whether the solitons are robust enough to evolve adiabatically in the medium without losing a great deal of their energy in the process or even being destroyed.

To predict that such is the case under experimentally feasible conditions and to study the dynamics of the process, we performed series of numerical simulations in which we solved relations (4) for a variety of material and input light conditions. Here we report our findings for the geometry in which the initial value of β is positive and reasonably large, and hence only FH light is input in the sample. In the simulations shown here we set $a_1(\xi = 0) = A\,\mathrm{sech}(r_\perp)$, $\beta(0) = 25$, and $\beta(L) = -5$, where L is the sample length in units of ξ. When we set $|\beta_0| \sim 500$ and an actual QPM period τ_0 of $\sim$20 μm, such values correspond to a domain-length deviation relative to τ_0 of $\sim$1.2 μm over the sample length.

First, we show the typical outcome for an ideally long sample ($L = 50$) that has a correspondingly slow variation of the mismatch. Figure 2 shows the variation of the fraction of energy and the width of the evolving FH and SH beams for representative input conditions. The adiabatic evolution of the solitons, which implies that they follow the properties of the family at the local wave-vector mismatch, is clearly visible. That is, power is converted to the SH and the beams are compressed, as predicted by Fig. 1. During the adiabatic reshaping, the solitons shed a small fraction of energy in the form of radiation, but because $\beta(\xi)$ is smooth such losses are negligible. The oscillations of the width of the generated SH beams occur in the transient region in which the soliton is formed out of the input. The adiabatic evolution takes place until the value of the local mismatch reaches the threshold for the soliton energy considered, something that in the conditions shown in Fig. 2 occurs beyond $L = 50$. Beyond that value the solitons enter the no-trapping regime, and the beams spread quickly owing to diffraction. Features similar to those shown in Fig. 2 were obtained for other values of the input energy flow and the initial and final values of $\beta(\xi)$.

For the adiabatic shaping that we are describing to be of potential practical importance, it has to occur under a variety of conditions with short-enough

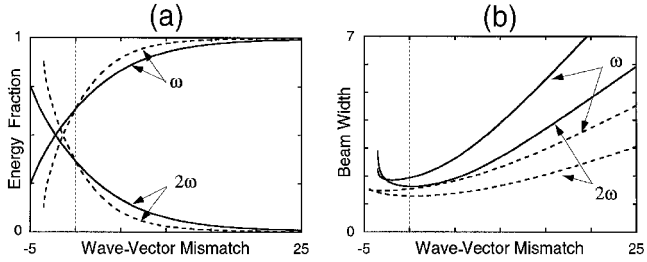

Fig. 1. Variation of the width (FWHM) and the fraction of energy carried by FH and SH beams forming a soliton with a given total energy flow as a function of wave-vector mismatch. Solid curves, $I = 15$; dashed curves, $I = 30$. Only stable solitons are plotted.

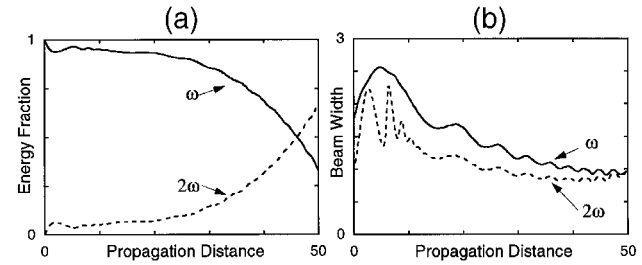

Fig. 2. Evolution of (a) the energy fraction and (b) the beam width of the energy for sample length $L = 50$. $A = 7$, $\beta(0) = 25$, and $\beta(L) = -5$. For a nominal QPM period of 20 μm, such values of β correspond to a domain length variation of $\sim$1.2 μm over the sample.

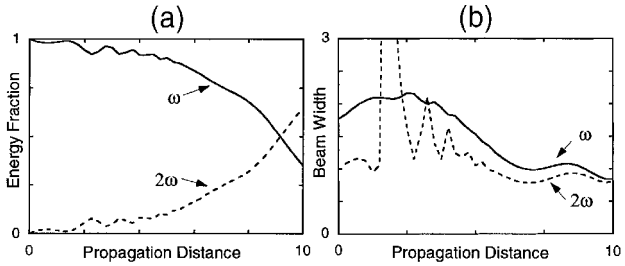

Fig. 3. Same as in Fig. 2 but for $L = 10$. For the experimental conditions discussed in the text, this corresponds to a sample length of ~2 cm.

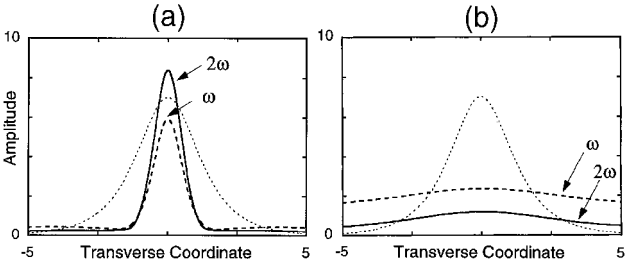

Fig. 4. Detail of the beam-amplitude profiles for the case $L = 10$. Solid curves, output SH; dashed curves, output FH; dotted curves, input FH. (a) Output of a chirped QPM sample. (b) Output of a sample with constant mismatch $\beta = -5$.

samples. To show that this indeed seems to be the case, next we present simulations for a sample with $L = 10$, which for the above values of the parameters corresponds to an actual length of ~2 cm. Figure 3 shows the outcome of a typical simulation. The figure shows that even in the presence of the much faster variation of $\beta(\xi)$ the beams follow the soliton families with no significant energy loss. Figure 4(a) shows the shapes of the input and output soliton beams.

The results of Figs. 2–4 correspond to almost the maximum variation of $\beta(\xi)$ and hence the strongest beam reshaping possible for the conditions considered. When the sought-after soliton shape corresponds to an intermediate value of $\beta(\xi)$, the soliton reshaping is weaker and thus more adiabatic. Also, here we have considered the simplest possible variation of the QPM domain lengths. Engineered higher-order QPM chirps in which, e.g., the period changes faster at the beginning of the sample than at the end might help to optimize the shaping process. For example, they might shorten the sample length required. Finally, a crucial point that needs to be stressed is that to excite the output solitons shown in Fig. 4(a) in a sample with a constant $\beta = -5$ with reasonable energy losses, both a FH and a strong coherent in-phase SH seed ought to be initially supplied. Otherwise, one gets the output shown in Fig. 4(b).

In conclusion, we have investigated the evolution of spatial solitons in properly tailored, chirped QPM samples made of quadratic nonlinear materials. We showed that one can use such a geometry to adiabatically shape the solitons into different beam profiles and widths or into different fractions of energy carried by each of the waves that form the solitons. Engineered higher-order QPM chirps might optimize the shaping process. Here we focused on spatial solitons in planar waveguides, but the idea can be extended to soliton propagation in bulk media, temporal solitons, light bullets, and quadratic solitons existing in optical cavities.

This study was supported by the Spanish Government under contract PB95-0768. We gratefully acknowledge support by the European Union and by the Centre de Supercomputacio de Catalunya through the Training and Mobility of Researchers program.

*Permanent address, Department of Mathematical Modelling, Technical University of Denmark, DK-2800 Lyngby, Denmark.

References

1. Yu. N. Karamzin and A. P. Sukhorukov, Sov. Phys. JETP **41,** 414 (1976).
2. For reviews, see G. I. Stegeman, D. J. Hagan, and L. Torner, Opt. Quantum Electron. **28,** 1691 (1996); K. Blow and G. Stegeman, eds., feature on nonlinear guided waves: physics and applications, J. Opt. Soc. Am. B **14,** 2950–3260 (1997).
3. W. E. Torruellas, Z. Wang, D. J. Hagan, E. W. Van Stryland, G. I. Stegeman, L. Torner, and C. R. Menyuk, Phys. Rev. Lett. **74,** 5036 (1995); R. Schiek, Y. Baek, and G. I. Stegeman, Phys. Rev. E **53,** 1138 (1996).
4. C. Etrich, U. Peschel, and F. Lederer, Phys. Rev. Lett. **79,** 2454 (1997).
5. C. Conti, S. Trillo, and G. Assanto, Phys. Rev. Lett. **78,** 2341 (1997); H. He and P. Drummond, Phys. Rev. Lett. **78,** 4311 (1997); T. Peschel, U. Peschel, F. Lederer, and B. A. Malomed, Phys. Rev. E **55,** 4730 (1997).
6. P. D. Drummond and H. He, Phys. Rev. A **56,** R1107 (1997); M. J. Werner and P. D. Drummond, Phys. Rev. A **56,** 1508 (1997).
7. L. Torner, C. R. Menyuk, and G. I. Stegeman, Opt. Lett. **19,** 1615 (1994); Opt. Commun. **114,** 136 (1995).
8. A. V. Buryak and Y. S. Kivshar, Opt. Lett. **19,** 1612 (1994); Phys. Lett. A **197,** 407 (1995).
9. H. H. Kuehl, J. Opt. Soc. Am. B **5,** 709 (1988); S. V. Chernikov, E. M. Dianov, D. J. Richardson, and D. N. Payne, Opt. Lett. **18,** 476 (1993).
10. M. M. Fejer, G. A. Magel, D. H. Jundt, and R. L. Byer, IEEE J. Quantum Electron. **28,** 2631 (1992).
11. M. A. Arbore, A. Galvanauskas, D. Harter, M. H. Chou, and M. M. Fejer, Opt. Lett. **22,** 1341 (1997).
12. L. Torner and G. I. Stegeman, J. Opt. Soc. Am. B **14,** 3127 (1997).
13. C. B. Clausen, O. Bang, and Y. S. Kivshar, Phys. Rev. Lett. **78,** 4749 (1997).